

Article

Analysis of Heat Insulation for Coil in the Electromagnetic Induction Controlled Automated Steel-Teeming System

Xian-Liang Li ^{1,2}, Ming He ^{1,3}, Xiao-Wei Zhu ^{1,3}, Qing-Wei Wang ^{1,3} and Qiang Wang ^{1,*}

¹ Key Laboratory of Electromagnetic Processing of Materials (Ministry of Education), Northeastern University, Shenyang 110819, China; lixianliang@stumail.neu.edu.cn (X.-L.L.); hemingepm@aliyun.com (M.H.); neuepmzxw@gmail.com (X.-W.Z.); wqw920708@163.com (Q.-W.W.)

² School of Materials Science and Engineering, Northeastern University, Shenyang 110819, China

³ School of Metallurgy, Northeastern University, Shenyang 110819, China

* Correspondence: wangq@mail.neu.edu.cn; Tel.: +86-024-8368-1726

Received: 15 February 2019; Accepted: 10 April 2019; Published: 12 April 2019



Abstract: Due to heat transfer of liquid steel, ambient temperature of induction coil in the electromagnetic induction controlled automated steel-teeming (EICAST) system is extremely high, which causes the coil damage and seriously restricts development of the EICAST technology. To solve the problem, a numerical simulation method was used to study the heat insulation effect of using different kinds, different thicknesses and different positions of heat insulation materials on induction coil. Finally, the optimum heat insulation method of induction coil was obtained and validated by experiments. The results show that after 10 mm heat insulation coating or 5 mm insulation coating +5 mm insulation felt was arranged on the outside of induction coil, the ambient temperature of the coil could be reduced to 614 °C and 589 °C, respectively. The two methods above can get the ideal heat insulation effect and meet the life requirements of induction coil for the EICAST technology.

Keywords: electromagnetic induction controlled automated steel-teeming (EICAST); induction heating; heat insulation; heat transfer; continuous casting

1. Introduction

Due to the use of nozzle sand during the steel-teeming process in continuous casting production, the steel cleanliness will be affected and the free opening rate of ladle cannot reach 100% [1–3]. Metallurgists [4–6] have done lots of work to reduce the pollution generated by nozzle sand to liquid steel and to improve the free opening rate, but they have not thoroughly avoided the use of nozzle sand. The Electromagnetic Induction Controlled Automated Steel-Teeming (EICAST) technology completely solves the drawbacks caused by the use of nozzle sand in traditional steel-teeming technology [7–11]. In this new technology, the nozzle sand is replaced by Fe-C alloy particles, whose composition is similar or the same as the liquid steel, and an induction coil located in nozzle brick is used to melt part or all of the sintered Fe-C alloy. However, the application bottleneck of this technology is found during the industrial test process. As a key device of the EICAST system, the induction coil needs to be installed inside the nozzle brick and to cycle with the ladle. According to the actual production process, the ladle needs to undergo baking, containing liquid steel, refining and the steel-teeming process. During the baking process, induction coil will bear heat transfer from the upside of nozzle brick at about 1000 °C for 2 h. When liquid steel in the ladle enters the refining stage, it will bear heat transfer not only from liquid steel on the upside of nozzle brick at 1600 °C for 2 h but also from the Fe-C sintered layer inside upper nozzle for 2 h. All of these will cause the ambient temperature of induction coil to remarkably increase before it works. As the ambient temperature increases, the resistance of induction

coil will also increase, which will lead to the power supply needing to output higher power to meet the induction heating requirement. During the steel-teeming process, induction coil will also bear heat transfer from liquid steel in the casting hole for 40 min. The induction coil has to service at least 30 thermal cycle times according to different production conditions. While the softening temperature of induction coil is only 650 °C [12], the structure strength and hardness of induction coil will decrease obviously when the temperature is higher than 650 °C. The performance of copper induction coil will be poor under thermal shocks repeatedly, which directly causes the coil damage and seriously restricts the wide industrial success of the EICAST technology.

To solve the problem of coil excessive high temperature in the EICAST system, He et al. [13] analyzed the heat condition of induction coil under different stages and obtained ambient temperature of induction coil by numerical simulation. It was found that the coil ambient temperature is 626 °C after heating at 1000 °C for 2 h and refining at 1600 °C for 2 h, and it reaches 791 °C after steel-teeming for 40 min. Liu et al. [14] found that high ambient temperature can be reduced by arranging heat insulation material on the outside of induction coil. The ambient temperature of induction coil can be reduced to 150 °C after arranging 40 mm vermiculite as a heat insulation layer outside the induction coil. Although arranging 40 mm vermiculite can achieve a better heat insulation effect, the thickness of 40 mm cannot meet the actual production requirements, and the safety has not been tested and analyzed. Currently, in order to meet the severe heat protection requirements, high temperature heat insulation material has achieved great development [15–20], new heat insulation materials represented by aerogel [21], nano heat insulation material [22], fiber heat insulation material [23] and heat insulation coating [24] are lighter and thinner, their heat insulation performances are better, which may provide new method to reduce the coil ambient temperature and to ensure the feasibility of the EICAST technology.

Therefore, a numerical simulation method is used in this paper to study the heat insulation effect of different kinds, different thicknesses and different arrangement methods of heat insulation material arranged for induction coil. Then, the optimal results of numerical simulation are verified by experiment, and the optimum heat insulations method to reduce the ambient temperature of induction coil is obtained.

2. Research Methods

2.1. Numerical Simulation

In this paper, the commercial software ANSYS (ANSYS 12.0, ANSYS Transient Thermal, ANSYS Inc., Pittsburgh, PA, USA) is applied to calculate the thermal field.

2.1.1. Model and Mesh

Figure 1a shows the model of nozzle brick in numerical simulation calculation, which is a reference to a steel plant. The front sectional elevation of nozzle brick and relevant sizes are shown in Figure 1b. The point A of induction coil in front view is its ambient temperature in numerical simulation. The meshing of the model is given in Figure 1c. The computational domain was discretized by using about 400,000 nonuniform tetrahedral/hexahedral grids. In particular, densely packed grids are applied to the coil, the heat insulation material, and the casting hole. In the process of calculation, the irrelevance of the number of grids and the time step has been discussed.

Some sizes of model are shown in Table 1, the casting hole (filled with Fe-C alloy particles) is a three circular truncated cone structure, and the parameter size in the table is the diameter of the upper surface of the circular table. The distance between the center of the casting hole and the center of the brick is 100 mm (both centers are on the longitudinal section of the center). The induction coil is made by a copper tube with a specification of $20 \times 20 \times 3 \text{ mm}^3$, the turn of induction coil is 6, the space between two turns is 5 mm, and the inner diameter is 235 mm.

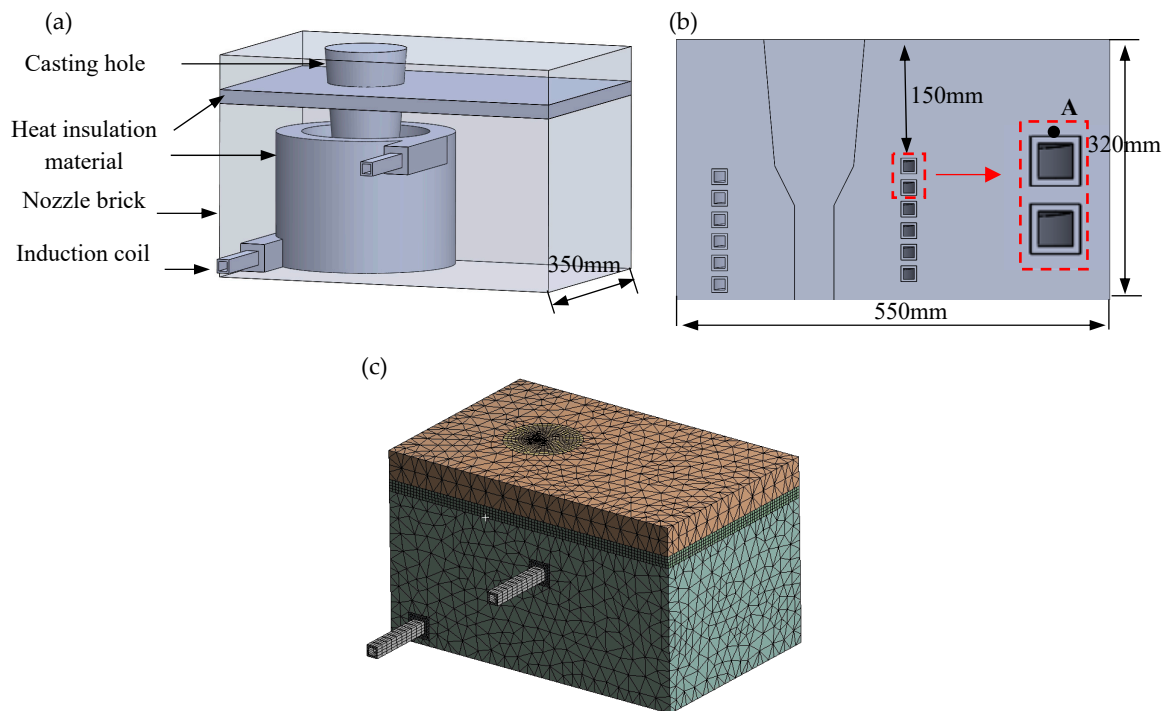


Figure 1. Simulation model: (a) three-dimensional model; (b) front sectional elevation; (c) mesh generation.

Table 1. Some sizes of models.

Parameter	Value/mm
Diameter and height of top circular truncated cone	128, 160
Diameter and height of middle circular truncated cone	10, 050
Diameter and height of bottom circular truncated cone	50, 140
Inner diameter of induction coil	235
Height of induction coil	150

2.1.2. Assumption

In order to reduce the amount of calculation, some assumptions are proposed:

- (1) Due to the heat transfer effect of the Fe-C alloy on coil temperature being constant under the same condition, the Fe-C alloy particles are well packed in the upper nozzle and the space between it can be neglected;
- (2) The upper nozzle working with the nozzle brick is neglected as a whole part of the nozzle brick;
- (3) The molten steel temperature is 1600 °C and initial environment temperature is 22 °C, and the adiabatic layer is around the nozzle brick.
- (4) There is air filling in induction coil and contact with the bottom of the nozzle brick, and the convective heat transfer coefficient is 5 W/(m²·°C) and 15 W/(m²·°C), respectively.

2.1.3. Governing Equations

In the case of the three-dimensional heat transfer process, partial differential equation of heat conduction as followed can be used in calculating:

$$\rho c \frac{\partial T}{\partial \tau} = \frac{\partial}{\partial x} \left(\lambda \frac{\partial T}{\partial x} \right) + \frac{\partial}{\partial y} \left(\lambda \frac{\partial T}{\partial y} \right) + \frac{\partial}{\partial z} \left(\lambda \frac{\partial T}{\partial z} \right), \quad (1)$$

where: ρ is the material density, kg/m³; c is the specific heat capacity, J/(kg·°C); T is the temperature, °C; τ is the time, s; λ is the thermal conductivity, and W/(m·°C).

2.1.4. Physical Parameters

Table 2 gives the physical parameters of the materials during numerical calculation. The thermal conductivity of heat insulation materials and air play a vital role in the induction coil heat insulation, and it is the focus of this paper. Therefore, the thermal conductivity of heat insulation materials and air varying temperature is given, and the thermal conductivity of three other materials does not change with temperature.

Table 2. Physical parameters of several materials.

Material	Density kg/m ³	Specific Heat Capacity J/(kg·°C)	Thermal Conductivity W/(m·°C)			
			400 °C	600 °C	800 °C	1000 °C
Nozzle brick	3040	1130			2.9	
Fe-C alloy	7830	550			24	
Induction coil (copper)	8300	385			401	
Air	1.165	1005	0.052	0.062	0.072	0.081
Mullite fiber blanket	128	800	0.09	0.13	0.176	0.22
Alumina fiber aerogel	330	500	0.02	0.025	0.042	0.055
Heat insulation coating	1200	500	0.038	0.049	0.061	0.068
Zirconium silicate porous felt	430	800	0.035	0.045	0.055	0.065

2.1.5. Boundary Conditions

The temperature curve, which is the load exerted on the brick, was designed according to a steel mill. Firstly, the upside of nozzle brick was heated to 1000 °C by 60 min and holding for 120 min, in order to imitate the baking stage of ladle. Then, the temperature was raised to 1600 °C by 30 min and holding for 120 min, in order to imitate the refining stage. Finally, the upper surface of nozzle brick and the inner surface of casting hole was heated to 1600 °C and holding for 40 min in the simulation, to imitate the steel-teeming stage. After the 40 min, it was cooled in free air to the room temperature.

2.2. Experiment

In order to simulate the real production situation in a steel plant and to compare the simulation results, an experimental platform was built in the laboratory. Figure 2 shows the schematic diagram of the platform. The upside of nozzle brick can be directly heated by resistance furnace, and the highest temperature can exceed 1600 °C, which can replace molten steel. Two heat insulation materials, heat insulation coating and heat insulation felt, were selected for induction coil to do experiments. After the heat insulation materials were arranged outside the induction coil, they were installed inside nozzle brick for thermal experiments. During the experiments, the first thing was to fill the Fe-C alloy particles into the casting hole. Then, the resistance furnace adjusted to right position was opened to heat the nozzle brick according to the temperature curve. Finally, during the heating process, the temperature was measured by a K-thermocouple which was arranged in the nozzle brick. We repeated the experiment for three times to ensure the accuracy.

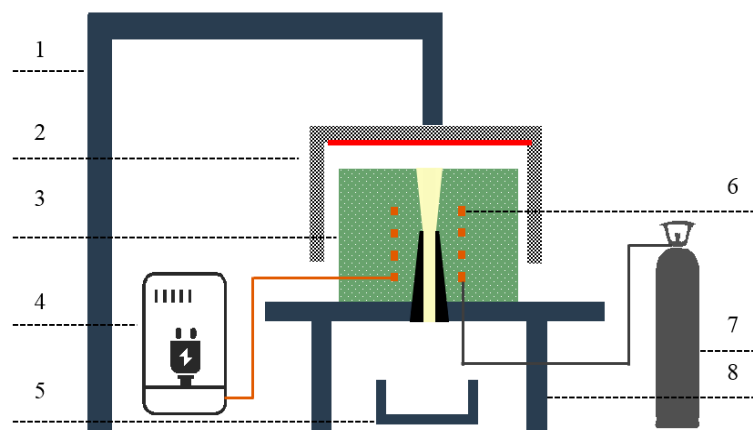


Figure 2. Schematic illustration of the EICAST experimental device. 1—Support structure; 2—Resistance furnace; 3—Nozzle brick; 4—Induction power supply; 5—Collecting device; 6—Induction coil; 7—Compressed air; 8—Experimental platform.

2.3. Validation of Numerical Simulation

The validation of numerical simulation can be found in our previous paper [13]. The ambient temperature of induction coil is calculated by numerical simulation and measured by experiment. Experimental results agree well with numerical simulation results after the upper surface of the brick reaches 1600 °C, as shown in Figure 3.

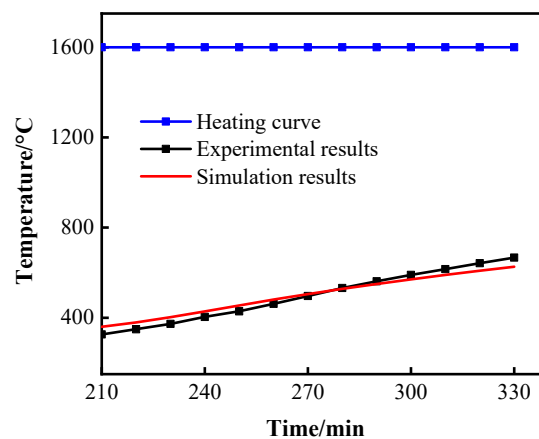


Figure 3. Temperature variation curve of coil ambient temperature.

3. Results and Discussion

3.1. Simulation Study on Effect of Heat Insulation Material Thickness

Heat insulation material thickness of the induction coil is limited by the sizes of nozzle bricks in the EICAST system. With the increase of the heat insulation material thickness, the strength of nozzle brick will decrease continuously. Therefore, ensuring the strength of nozzle brick, the influence of using 4, 6, 8 and 10 mm heat insulation coating on induction coil temperature is analyzed, respectively. Figure 4 presents induction coil temperature before and after steel-teeming stage ($t = 330$ min and 370 min) with different coating thicknesses.

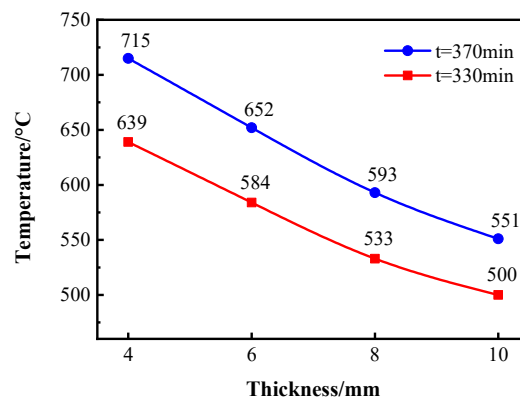


Figure 4. Induction coil temperature before and after steel-teeming stage with different coating thicknesses.

Figure 4 shows that the ambient temperature of induction coil can be obviously reduced by arranging heat insulation coating. With the increase of coating thickness, the ambient temperature of induction coil decreases. Comparing induction coil temperature at $t = 330$ min and 370 min, it can be seen that the temperature difference of 10 mm thickness is the smallest, and as the thickness increases, the ability of the heat insulation material to resist external temperature changes also increases. Accordingly, in order to achieve the best heat insulation effect, under the premise of ensuring that the strength of the brick, the 10 mm thickness is selected to use in the following.

3.2. Simulation Study on the Effect of Heat Insulation Material Arrangement Methods

Figure 5 displays the ambient temperature of induction coil when the heat insulation coating is arranged by three ways. The arrangement methods are on the outside of induction coil (I), on the upside of induction coil (II) and the combination of above two methods (III). When the coating is arranged on the upside of induction coil, the coating thickness is 20 mm, and the length from the upside of nozzle brick to the coating is 50 mm. It can be concluded that the heat insulation effect of methods I and II are basically similar before $t = 330$ min. When the heat insulation material is arranged on the upside of the induction coil, the ambient temperature of the induction coil rises sharply after $t = 330$ min. The reason is that this heat insulation method cannot resist the heat transfer from liquid steel in the casting hole during the steel-teeming stage. The ambient temperature of induction coil is reduced to 360 °C by method III. In this way, the coating arranged on the upside of induction coil can resist the heat transfer from liquid steel at the upside of nozzle brick, and the coating arranged on the outside of induction coil can resist the heat transfer not only from liquid steel on the upside of nozzle brick but also in the casting hole. Therefore, the coil temperature can be significantly reduced by method III.

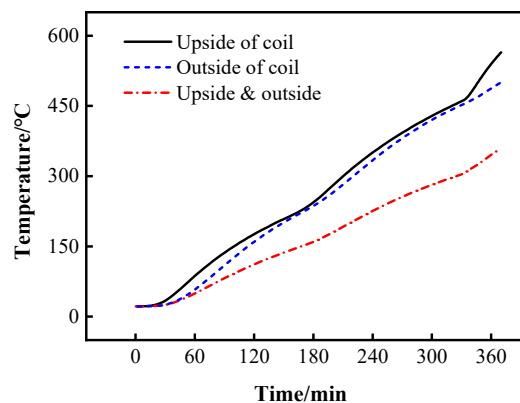


Figure 5. Induction coil temperature with different heat insulation material arrangement methods.

Figure 6 illustrates the temperature distribution of nozzle brick at 330 min and 370 min after using three heat insulation methods. Figure 6a,b demonstrate that the ambient temperature of the induction coil can be reduced by arranging heat insulation material on the outside of induction coil; Figure 6c presents that heat insulation material arranged on the upside of induction coil can resist the heat transfer from liquid steel before steel-teeming; Figure 6b,d present that the heat transfer of liquid steel in casting hole is obvious when the heat insulation material is only arranged on the upside of the induction coil; Figure 6e,f present that the ambient temperature of the induction coil can be reduced significantly by arranging heat insulation material on both the outside and upside of induction coil. However, the external temperature of the heat insulation material in method III is higher than that in the previous two methods. The reason for this phenomenon is that the ambient temperature of induction coil can be reduced by arranging heat insulation material, and the decreased heat has to be transferred through other media with high thermal conductivity outside the heat insulation material.

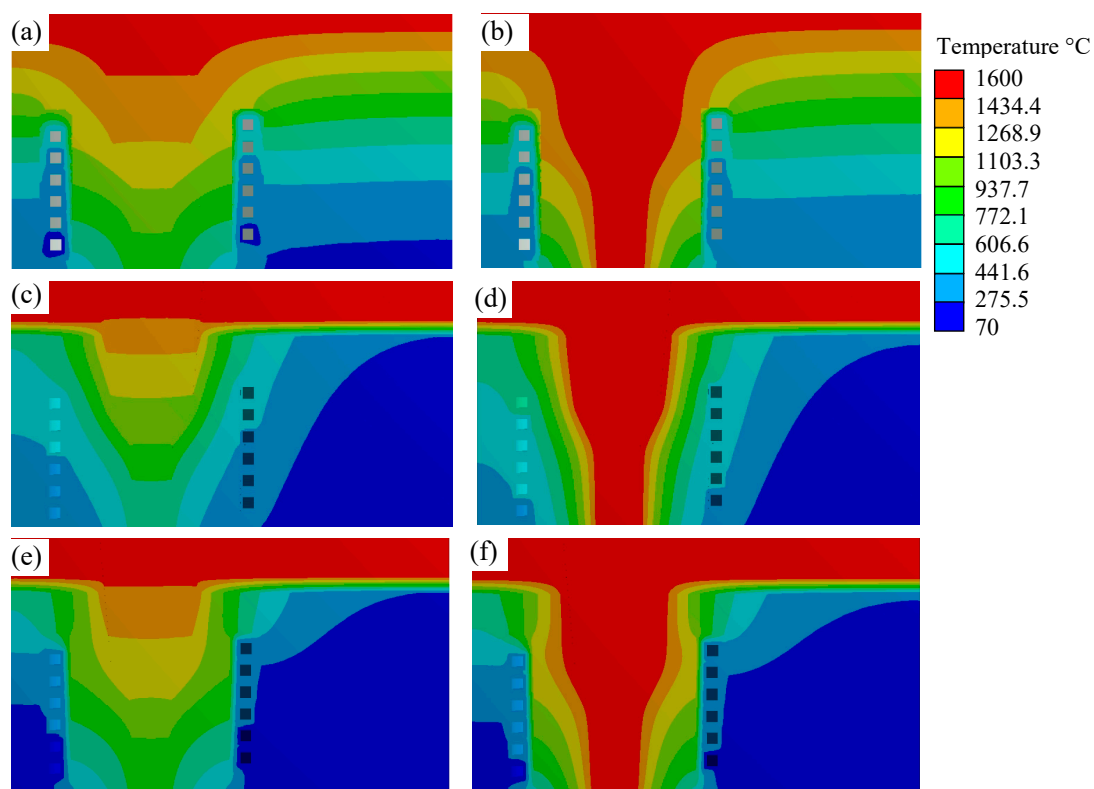


Figure 6. Temperature distribution of nozzle brick: method I (a) $t = 330$ min; (b) $t = 370$ min; method II; (c) $t = 330$ min; (d) $t = 370$ min; method III; (e) $t = 330$ min; (f) $t = 370$ min.

Although the heat insulation material arranged on the upside of induction coil can reduce the ambient temperature of induction coil, there are still two drawbacks in this method. Firstly, the results given in Figure 6 manifest that the external temperature of heat insulation material is about 1400 °C, which exceeds the limit temperature of heat insulation material. Secondly, the heat insulation material cannot be arranged in the brick according to the geometric model; the nozzle brick will be divided into two parts. Numerical simulation results provide different ways of heat insulation material arrangement for induction coil, but the arrangement method of the heat insulation material on the upside of induction coil is not yet mature.

3.3. Simulation Study on the Effect of Heat Insulation Materials

The induction coil in the EICAST system is a special-shaped workpiece, ordinary plate and block heat insulation materials are not suitable to be placed on the outside of the induction coil. The heat

insulation coating can be directly coated and the flexible heat insulation material can be covered on the outside of the induction coil. Therefore, the effect of heat insulation materials including heat insulation coating and three kinds of flexible heat insulation materials (aerogel felt, zirconium silicate porous felt and mullite fiber blanket) arranged on the outside of induction coil in the EICAST system are analyzed.

After steel-teeming for 40 min ($t = 370$ min), the temperatures outside the induction coil and four different heat insulation materials are shown in Figure 7. It can be observed that the heat insulation effect of the aerogel felt is the best and the mullite fiber blanket is the worst. The zirconium silicate porous felt and coating have a similar heat insulation effect. According to numerical simulation results, aerogel felt should be the best choice of heat insulation material, but the aerogel felt is still in the research and development stage, its maximum use temperature is about 650 °C [25]. Figure 7 indicates the external temperature of aerogel felt has reached 856 °C, so it is not suitable for the EICAST system. The zirconium silicate porous felt can reduce the temperature from 902 °C to 475 °C, the temperature difference is 427 °C, and the temperature difference of heat insulation coating is 343 °C. Thus, the heat insulation effect of zirconium silicate porous felt is better. However, the external temperature of coating is lower than that of zirconium silicate porous felt, and its unique construction technology is suitable for brushing on the outer surface of induction coil. Therefore, the coating and zirconium silicate porous felt (heat insulation felt) are selected for further experiments to analyze the heat insulation performance.

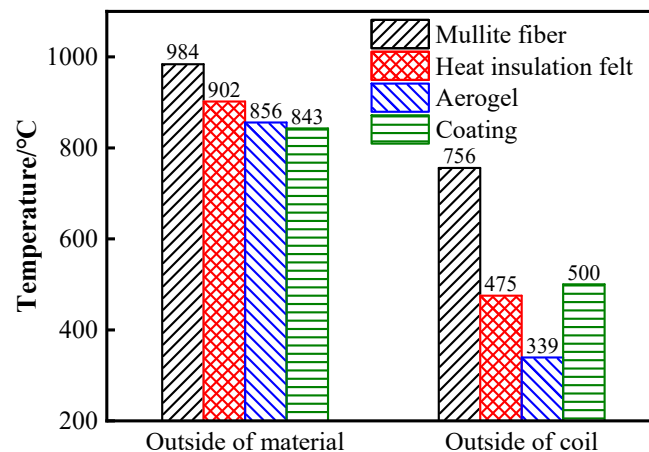


Figure 7. Heat insulation effect of different heat insulation materials at $t = 370$ min.

3.4. Experimental Study on Different Heat Insulation Methods of Induction Coil

Numerical simulation results denote that the 10 mm heat insulation coating or heat insulation felt are suitable for the EICAST system by arranging on the outside of induction coil. Two heat insulation materials, 10 mm heat insulation coating and 10 mm insulation felt, are used in the experiments. In addition, the effect of the combination of two heat insulation materials on the induction coil temperature is also analyzed. Therefore, three different experiments are carried out as follows: (1) 10 mm heat insulation coating; (2) 10 mm heat insulation felt; (3) 5 mm heat insulation coating +5 mm insulation felt.

Figure 8 demonstrates the induction coil temperature after arranging 10 mm heat insulation coating and 10 mm heat insulation felt on the outside of induction coil. The experimental result error is less than 20 °C by repeating three times, which indicates that the two heat insulation materials are stable and can resist repeated thermal shock. After the upside temperature of nozzle brick is 1600 °C for 2 h, the temperature difference of 10 mm insulation felt is bigger, so its heat insulation effect is better than that of the heat insulation coating theoretically. However, the final coil (614 °C) temperature of using heat insulation coating is lower than that of using the heat insulation felt (683 °C); the reason is that the heat insulation felt has lower density and higher specific heat capacity. Therefore, for reducing the ambient temperature of induction coil, 10 mm heat insulation coating is more suitable for the EICAST system. In addition, the external temperature of 10 mm heat insulation felt reaches 1117 °C,

which exceeds the limit temperature of heat insulation felt (1100 °C), so using heat insulation felt alone is not applicable to the EICAST system.

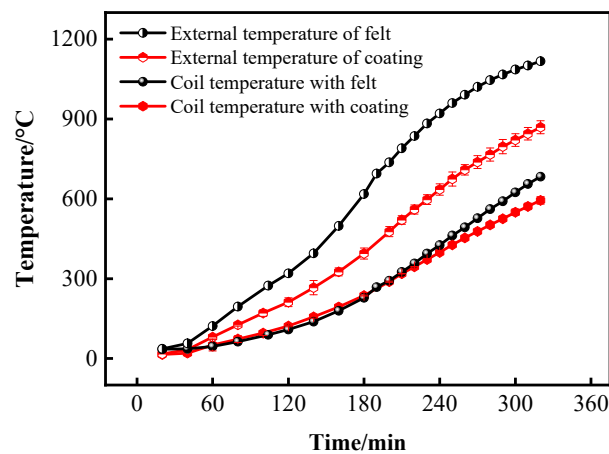


Figure 8. Temperature of the induction coil after arranging 10 mm coating and heat insulation felt.

In numerical simulation, the performance of heat insulation felt is better than that of heat insulation coating, but, in the experiment, the opposite results are obtained. The main reasons are as follows: (1) the heat insulation coating, as a functional coating, can be directly coated on the outside of induction coil, but the heat insulation felt can only be covered on it. The numerical simulation model cannot reflect the difference of the results caused by the material characteristics; (2) the insulation felt thickness specification is 5 mm, so induction coil has to be covered by double heat insulation felt layers, the contact heat transfer between two layers is neglected during the simulation process.

Figure 9 illuminates the temperature of the induction coil when 5 mm heat insulation coating and 5 mm insulation felt are arranged on the outside of the induction coil. After the upside temperature of nozzle brick is 1600 °C for 2 h, the external temperature of heat insulation felt is 968 °C, induction coil temperature is 589 °C, and the temperature difference is 379 °C, which is 102 °C higher than that of the heat insulation coating. By this method, the temperature difference can be improved significantly. In addition, the actual heat insulation effect for induction coil is improved. The ambient temperature of the induction coil is reduced from 614 °C to 589 °C and the decreased temperature is 25 °C.

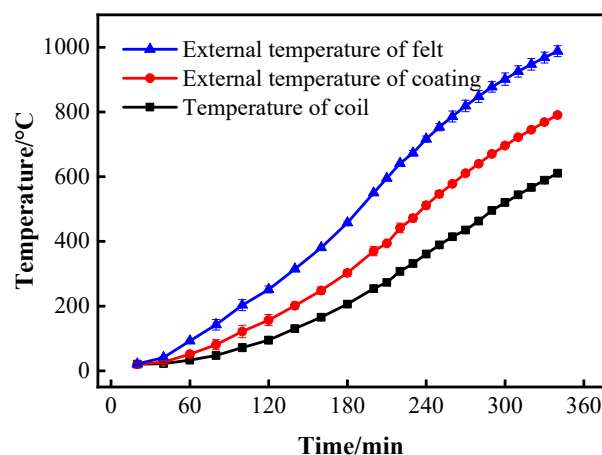


Figure 9. Induction coil temperature after arranging 5 mm heat insulation coating and 5 mm insulation felt.

Figure 10 exhibits the comparison of the heat insulation effect among three heat insulation methods. The temperature of the horizontal line is the softening temperature of the copper coil (650 °C). All three ways can reduce induction coil temperature. The effect of the 10 mm heat insulation felt is relatively

bad, the ambient temperature exceeds the softening temperature, and external temperature of heat insulation felt exceeds its limit use temperature. In addition, 10 mm heat insulation coating can reduce the ambient temperature obviously, and external temperature of the insulation material is lower than its limit use temperature. The heat insulation performance of 5 mm coating +5 mm insulation felt is the best, which can reduce the ambient temperature to 589 °C, and the external temperature of heat insulation material is less than 1000 °C. In addition, through the method of combination of heat insulation coating and heat insulation felt, the advantages of coating, such as good adhesion, the fact that the coating does not easily fall off and has long service life, are achieved, and the characteristics of heat insulation felt are also realized. To sum up, a perfect heat insulation effect can be acquired by arranging 10 mm insulation coating or 5 mm insulation coating +5 mm insulation felt on the outside of induction coil. Both methods meet the requirements of induction coil service life in the EICAST technology.

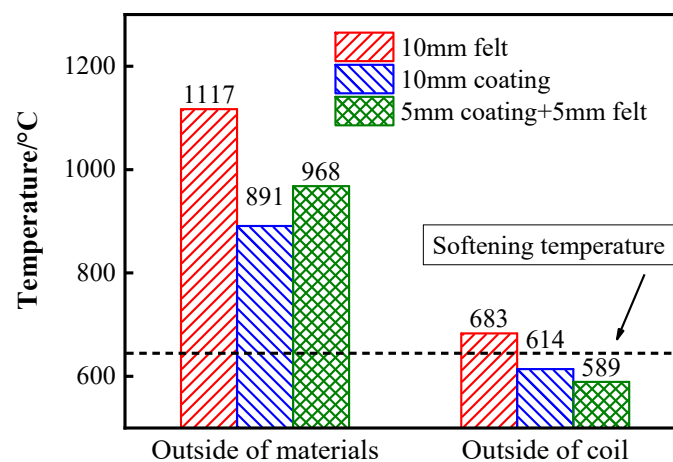


Figure 10. Effect comparison of three heat insulation methods.

4. Conclusions

(1) The heat insulation coating and zirconium silicate porous felt are suitable for heat insulation of induction coil, and when the heat insulation material thickness is 10 mm, it will not change the strength of nozzle brick, and can achieve a good heat insulation effect.

(2) The ambient temperature of induction coil can be reduced by arranging the heat insulation materials on the outside and upside of induction coil. However, when the insulation layer is arranged on the upside of induction coil, the structure of nozzle brick will be changed and the external temperature of heat insulation material exceeds its limit use temperature. Therefore, heat insulation materials arranged on the outside of induction coil are more suitable for the EICAST technology.

(3) When 10 mm insulation coating is arranged on the outside of induction coil, the ambient temperature is 614 °C after upside temperature of nozzle brick is 1600 °C for 2 h, and it can be reduced to 589 °C by arranging 5 mm insulation coating +5 mm insulation felt. Both the two methods can achieve admirable heat insulation effect, and they meet the requirements of induction coil service life in the EICAST technology.

Author Contributions: Q.W. conceived and designed the experiments, X.-L.L. analyzed the data and wrote the paper, M.H. and Q.-W.W. performed the experiments, and X.-W.Z. provided valuable suggestions of the revision.

Funding: This research was supported by the National Natural Science Foundation of China (Grant No. U1560207) and the Liaoning Innovative Research Team in University (Grant No. LT2017011).

Conflicts of Interest: The authors declare no conflict of interest.

References

1. Zhang, L.F.; Thomas, B.G. State of the art in evaluation and control of steel cleanliness. *ISIJ Int.* **2003**, *43*, 271–291. [[CrossRef](#)]
2. Deng, Z.Y.; Glaser, B.; Bombeck, M.A.; Sichen, D. Effects of temperature and holding time on the sintering of ladle filler sand with liquid steel. *Steel Res. Int.* **2016**, *87*, 921–929. [[CrossRef](#)]
3. Kobayashi, Y.; Todoroki, H.; Kirihara, F.; Nishijima, W.; Komatsubara, H. Sintering behavior of silica filler sands for sliding nozzle in a ladle. *ISIJ Int.* **2014**, *54*, 1823–1829. [[CrossRef](#)]
4. Yang, J. A Device for Preventing Nozzle Sand Entering into Continuous Casting Tundish. Chinese Patent Appl. 201410634602.2, 27 October 2014.
5. Liu, W.D. A Method for Eliminating Nozzle Sand Used in Ladle. Chinese Patent Appl. 201110122547.5, 12 May 2011.
6. Liu, Z.Y.; Liu, G.X.; Sun, H.Y.; Song, L.F.; Chen, Z.Y.; Chen, X.L.; Wang, D.; Fan, S.W. External Connection Device for Big Ladle Drainage and Big Ladle Drainage Method of External Connection Device. Chinese Patent Appl. 201510972071.2, 2 December 2015.
7. Li, D.J.; Wang, Q.; Liu, X.A.; Gao, A.; Wang, X.B.; Dong, J.; Marukawa, M.K.; He, J.C. A new steel teeming technology by using electromagnetic induction heating system in ladle. *J. Iron Steel Res. Int.* **2012**, *19*, 766–770. [[CrossRef](#)]
8. Wang, Q.; Li, D.J.; Liu, X.A.; Wang, X.B.; Dong, J.; He, J.C. Effects of steel teeming in new slide gate system with electromagnetic induction. *J. Iron Steel Res. Int.* **2015**, *22*, 30–35. [[CrossRef](#)]
9. Wang, Q.; He, M.; Zhu, X.W.; Li, X.L.; Wu, C.L.; Dong, S.L.; Liu, T. Study and development on numerical simulation for application of electromagnetic field technology in metallurgical processes. *Acta Metall. Sin.* **2018**, *54*, 228–246. [[CrossRef](#)]
10. He, M.; Wang, Q.; Liu, X.A.; Shi, C.Y.; Liu, T.; He, J.C. Analysis of power supply heating effect during high temperature experiments based on the electromagnetic steel teeming technology. *High Temp. Mater. Proc.* **2017**, *36*, 441–445. [[CrossRef](#)]
11. He, J.C.; Marukawa, K.; Wang, Q. Ladle with Steel Heating and Tapping Set and Its Tapping Method. Chinese Patent Appl. 200610045875.9, 2 August 2006.
12. Suzuki, H.; Kanno, M.; Maeda, T. Effects of small amounts of additive elements on softening temperature and electrical resistivity of cold-worked pure copper. *J. Jpn. Inst. Met.* **1983**, *47*, 794–801. [[CrossRef](#)]
13. He, M.; Li, X.L.; Liu, X.A.; Zhu, X.W.; Liu, T.; Wang, Q. Coil Ambient Temperature and Its Influence on the Formation of Blocking Layer in the Electromagnetic Induction-Controlled Automated Steel-Teeming System. *Acta Metall. Sin-Engl.* **2019**, *32*, 391–400. [[CrossRef](#)]
14. Liu, X.A.; Wang, Q.; Liu, T.; He, J.C. Analysis of working temperature of coil used in electromagnetic induction controlled automatic steel-teeming system. *J. Northeast. Univ.* **2014**, *35*, 51–55. [[CrossRef](#)]
15. Cheng, E.J.; Sakamoto, J.; Salvador, J.; Wang, H.; Maloney, R.; Thompson, T. Cast-in-place, ambiently-dried, silica-based, high-temperature insulation. *Acta Mater.* **2017**, *127*, 450–462. [[CrossRef](#)]
16. Yuan, K.K.; Wang, X.Q.; Liu, H.J.; Feng, C.; Liu, B.X.; Cai, N.N.; Lin, X.J.; Zhi, L.Y.; Zhang, G.H.; Xu, D. Formation of barium zirconate fibers for high-temperature thermal insulation applications. *J. Am. Ceram. Soc.* **2016**, *99*, 2913–2919. [[CrossRef](#)]
17. Salomão, R.; Bôas, M.V.; Pandolfelli, V. Porous alumina-spinel ceramics for high temperature applications. *Ceram. Int.* **2011**, *37*, 1393–1399. [[CrossRef](#)]
18. Xie, T.; He, Y.L.; Hu, Z.J. Theoretical study on thermal conductivities of silica aerogel composite insulating material. *Int. J. Heat Mass Transf.* **2013**, *58*, 540–552. [[CrossRef](#)]
19. Ruckdeschel, P.; Philipp, A.; Retsch, M. Understanding thermal insulation in porous, particulate materials. *Adv. Funct. Mater.* **2017**, *27*, 1702256:1–1702256:11. [[CrossRef](#)]
20. Shang, L.; Wu, D.F.; Pu, Y.; Wang, H.T.; Gao, Z.T. Experimental research on thermal insulation performance of lightweight ceramic material in oxidation environment up to 1700 °C. *Ceram. Int.* **2016**, *42*, 3351–3360. [[CrossRef](#)]
21. Lee, J.K.; Gould, G.L.; Rhine, W. Polyurea based aerogel for a high performance thermal insulation material. *J. Sol-Gel Sci. Technol.* **2009**, *49*, 209–220. [[CrossRef](#)]
22. Akamine, S.; Fujita, M. Controlling heat radiation for development of high-temperature insulating materials. *J. Eur. Ceram. Soc.* **2014**, *34*, 4031–4036. [[CrossRef](#)]

23. Lee, S.C.; Cunnington, G.R. Conduction and radiation heat transfer in high-porosity fiber thermal insulation. *J. Thermophys. Heat Transf.* **2012**, *14*, 121–136. [[CrossRef](#)]
24. Dai, L.; Feng, J.; Wang, Y.W. High-Temperature-Resisting Heat-Insulation Coating as well as Preparation Method and Application Thereof. Chinese Patent Appl. 201410004677.2, 6 January 2014.
25. He, Y.L.; Xie, T. Advances of thermal conductivity models of nanoscale silica aerogel insulation material. *Appl. Therm. Eng.* **2015**, *81*, 28–50. [[CrossRef](#)]



© 2019 by the authors. Licensee MDPI, Basel, Switzerland. This article is an open access article distributed under the terms and conditions of the Creative Commons Attribution (CC BY) license (<http://creativecommons.org/licenses/by/4.0/>).